Proceedings of the 2023 Design of Medical Devices Conference
DMD2023
April 17-19, 2023, Minneapolis, MN, USA

DMD2023

DESIGN OF A HYBRID-INERTIAL DEVICE FOR THE SEPARATION OF CIRCULATING TUMOR CELLS

Mohammed Raihan Uddin
Department of Mechanical Engineering
School of Engineering and Computer Science,
Washington State University
Vancouver, WA, United States

Dr. Xiaolin Chen
Department of Mechanical Engineering
School of Engineering and Computer Science,
Washington State University
Vancouver, WA, United States

ABSTRACT

Circulating tumor cells (CTCs) are shed from primary tumors, circulate in the bloodstream and are capable of initiating metastasis at distant anatomical sites. The detection and molecular characterization of CTCs are pivotal for early-stage cancer diagnosis and prognosis. Recently, microfluidic technology has achieved significant progress in the separation of cells from complex and heterogeneous mixtures for many biomedical applications. Conventional microfluidic platforms exploit the difference in size between the particles to achieve separation, which makes them ineffective for sorting overlapping-sized CTCs. To address this issue, we propose a method using a spiral channel for label-free, and high throughput separation of CTCs coupling Dielectrophoresis (DEP) with inertial microfluidics. A numerical model has been developed to investigate the separation effectiveness of the device over a range of electrical voltage and flow rates. The presented channel is shown to effectively isolate similar-sized CTCs from the white blood cells (WBCs) in a single-stage separation process. Subsequently, optimum working parameters to enhance separation efficiency have been proposed. The hybrid microfluidic device can provide valuable insight into the development of a robust, inexpensive, and efficient platform for cell separation with reduced analysis time for future cancer research and treatment.

Keywords: Place any keywords here

1. INTRODUCTION

Cancer is the second leading cause of death in the United States, and it causes approximately eight million deaths each year worldwide [1]. There is numerous ongoing research on the care strategy for cancer patients which includes early-stage diagnosis and treatment of cancer. One promising direction in the field of cancer research involves the isolation and detection of Circulating Tumor Cells (CTCs). CTCs are malignant cells shed into the bloodstream from a tumor that has the potential to establish metastases at different sites within the body. CTCs can act as biomarkers that have antigenic and genetic characteristics of the tumors it is shed from and can be extracted non-invasively from cancer patients using liquid biopsy [2]. CTCs can provide key biological information required for the diagnosis of cancer at an early stage and can be used as a tool to provide personalized medicine to patients [3]. However, CTCs occur at very low concentrations, e.g., a single tumor cell in a background of millions of blood cells [4]. In addition to that WBCs share many properties in common with CTCs. Therefore, the effective identification and characterization of CTCs from blood cells require devices of high analytical specificity [5].

Microfluidic technology has emerged as a promising solution for the separation of CTCs from blood cells. It is capable of separating cells of interest from a complex and heterogeneous mixture. Microfluidic separation techniques can mainly be classified into active and passive methods. Active methods such as dielectrophoresis (DEP), magnetophoresis and acoustophoresis utilize external force fields such as electric, magnetic, and acoustics respectively to achieve cell separation[6]. Generally, active microfluidic devices can precisely control particles of interest and adjust their position in real-time. However, such devices suffer from low throughput because of the long residual time. On other hand, passive methods such as inertial microfluidics, pinched flow fractionation (PFF), and deterministic lateral displacement (DLD) do not utilize any external fields and use only the inherent channel geometry or intrinsic hydrodynamic forces based on the size and deformability of the cells to manipulate them [7]. Among the passive devices, inertial microfluidics has gained much popularity due to its simple structure, robustness, and higher throughput separation of cells. Inertial microfluidics separate cells based on the inertial force acting on them. The

magnitude of this inertial force is largely dependent on the size of the cells [8]. Recent studies suggest that CTCs may have a significant size overlap with WBCs [9]. Therefore, a high level of WBCs contamination may be observed in the passive inertial devices.

To overcome the shortcomings of active and passive devices, hybrid techniques have been proposed that combine both active and passive methods. Hybrid devices offer design flexibility and specificity of the active device whereas maintaining the robustness and high-throughput nature of the passive devices[6]. Thus, a hybrid microfluidic device provides a more powerful and versatile cell sorting platform. A hybrid separation device using active DEP force and exploiting the inherent difference in the dielectric properties of the CTCs and the WBCs has demonstrated effective separation of the tumor cells from the blood cells. Rahmati et. al. [10] have combined DEP with passive deterministic lateral displacement (DLD) for the separation of breast cancer cells from the WBCs. However, the use of DLD limits the throughput of the device and increases the chance of clogging. Church et. al. [11] and Zhu et. al. [12] utilized DEP induced by the curvature in the channel for the electro-kinetic separation of the particles based on their size. Moon et. al. [13]utilized a combination of multi-orifice flow fractionation (MOFF) and DEP connected serially to separate breast cancer cells from blood samples. Separation of particles based on their size has also been achieved by Zhang et. al. [14] in a fully coupled inertial DEP serpentine channel. Additionally, Khan et. al. [15] studied the separation of CTCs from the WBCs in a similar electrode-embedded serpentine channel. However, separation is achieved in these devices using DEP forces at a high AC electric field voltage which may result in the electro-destruction of the cells.

To separate CTCs from similar-sized WBCs, a label-free method is proposed in this work coupling inertial microfluidics and DEP using a spiral microchannel. In this study, at first, the effects of the DEP force on separation of cells is investigated. Then the effects of the sheath flow and the flow rate are examined for the effective separation of the CTCs from the WBCs.

2. THEORY

At the low Reynolds number (Re < 1) flow the cells maintain their flow path in accordance with the fluid streamline. This is called Stokes flow or the creeping motion. However, the flow no longer functions in the Stokes regime for a moderately high Reynolds number of 1-100 because the particles deviate from their initial flow trajectory. Inertial microfluidics operates in this regime where the cells migrate laterally to multiple equilibrium positions due to the finite inertia of the fluid at a higher Reynolds number [8].

Cells randomly dispersed in a microchannel operating in an inertial regime will migrate to their equilibrium positions by the action of several forces [16]. First, the viscous drag force causes the cells to travel with the flow in the flow direction. Second, the lateral migration of the particles is caused by the counteracting effect of two opposing forces, namely shear-induced lift force, and wall-induced lift force. Due to the parabolic nature of the fluid velocity profile, shear-induced lift force causes a particle to migrate away from the center of the microchannel. On the other hand, the disturbance of the flow field around the cell, while it is in close vicinity to the wall gives rise to the asymmetric wake around the cell. This results in the wall-induced lift force which causes the cell to migrate from the wall to the center of the channel. The balance between these two opposing forces known as the net inertial lift force is given by the equation below[8]:

$$F_{Lift} = \frac{f_L \rho_f v_m^2 a_p^4}{D_h^2} \quad (1)$$

where, ρ_f is the fluid density, v_m is the maximum velocity of the fluid, a_p is the cell diameter and D_h is the hydraulic diameter of the channel and f_L is the lift coefficient which is a function of the Reynold number and vertical position of the cell within the channel. Additionally in a curved microchannel, a secondary flow can be observed at the crosssection of the channel due to the difference in momentum at the center of the channel and the near wall region. This secondary flow results in Dean drag which is given by the equation below [17]:

$$F_{Dean} = 5.4 \times 10^{-4} \pi \mu a_p De^{1.63} \quad (2)$$

The interdigitated electrodes placed at the bottom of the channel create a non-uniform electric field which causes the cells to experience dielectrophoretic (DEP) force which is given by the equation below [18]:

$$\boldsymbol{F_{DEP}} = 2\pi \varepsilon_{med} \left(\frac{a_p}{2}\right)^3 Re[K_{CM}(\omega)] \nabla |\boldsymbol{E}|^2 \quad (3)$$

where ε_{med} is the permittivity of the suspension medium, ω is the field frequency and $|\boldsymbol{E}|$ is the root-mean-squared intensity of the applied electric field. In the equation, $Re[K_{CM}(\omega)]$ represents the magnitude of the real part of the Clausius-Mossotti (CM) factor. The CM factor reflects the polarizability contrast between the cell and its suspension medium, and it is dependent on the frequency of the applied field. It can be seen from the equation above that the magnitude and direction of the DEP force are dependent on the real part of the CM factor. The cells are either attracted to the electrodes or repelled away from the electrodes when the DEP force is either positive or negative respectively. Between the negative and the positive DEP force, there exists a point where no DEP force acts on the cells and the CM factor is zero [19]. The frequency at which this occurs is called the cross-over frequency [20]. The migration of the cell at the influence of the inertial lift force, dead drag force, and DEP force can be exploited to achieve high throughput separation of the cells from the binary mixture.

3. OPERATING PRINCIPLE

In this work, CTCs are separated from WBCs by utilizing hybrid DEP inertial microfluidics. Lung cancer cells or A549 cells are considered to be the representative of CTCs as it has significant

size overlaps with the blood cells and Granulocytes are considered to be the representative of the WBCs as they make up for the largest portions of the WBCs found in an adult body [21]. The properties of the cells used in the simulations are summarized in Fig. 1. The values are obtained for a medium of conductivity of 0.055 S/m and relative permittivity of 80. To characterize the inhomogeneity due to the presence of different components within a cell a single shell model is used. In this study, an AC electric field matching the cross-over frequency of the CTC is applied [20]. At this frequency, the cancer cells experience no DEP force whereas the WBCs experience a negative DEP force which pushes them vertically upward away from the planar interdigitated electrodes placed at the bottom of the spiral microchannel. The electrodes have a width and gap of 100 µm and 20 µm respectively. The spiral microchannel shown in Fig. 2 has a rectangular cross-section of width and height of 300µm x 100µm respectively along with two inlets and two outlets. The sample along with a top sheath flow is pumped through the outer inlet. The top sheath flow pushes the cells in the sample toward the bottom of the channel. An additional sheath flow is pumped through the inner inlet which pushes the cells toward the outer wall of the spiral microchannel.

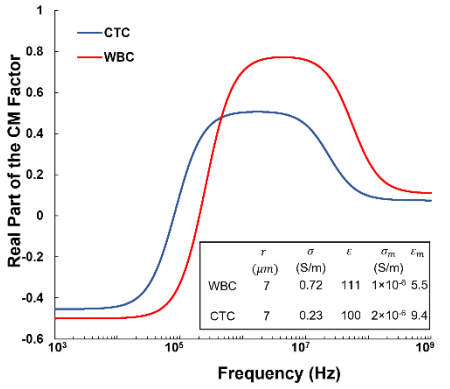

FIGURE 1: REAL PART OF THE CLAUSIUS-MOSSOTTI (CM) FACTOR FOR CTCS AND WBCS. THE PROPERTIES OF BOTH THE CELL TYPES USED IN THE STUDY ARE LISTED IN THE TABLE [10,20].

In this study, the velocity and pressure field has been obtained by solving the Navier-Stokes equation expressed below:

$$\rho\left[\frac{\partial \boldsymbol{v}}{\partial t} + \boldsymbol{v}.\nabla\boldsymbol{v}\right] = \nabla.\left[-pI + \mu\left(\nabla v + (\nabla v)^T\right)\right] \quad (4)$$

$$\nabla.\boldsymbol{v} = \boldsymbol{0} \quad (5)$$

where $\rho, \boldsymbol{v}, p,$ and μ are fluid density, velocity, pressure, and viscosity respectively. The nonuniform electric field generated by the electrodes is obtained by solving the following equations:

$$\boldsymbol{E} = -\nabla\phi \quad (6)$$

$$\nabla.(\varepsilon_m \boldsymbol{E}) = \rho_E \quad (7)$$

$$\frac{\partial \rho_E}{\partial t} + \nabla.(\boldsymbol{E}) = 0 \quad (8)$$

where ϕ, ε_m, ρ_E and σ are electric potential, medium permittivity, volumetric free charge density, and medium conductivity respectively. After velocity, pressure, and the non-uniform electric field have been obtained, a transient solver is used to determine the trajectories of the cells. The inertial lift forces, the dean drag, and the DEP force determine the motion of the particles, and all these forces are combined in Newton's second law of motion to determine the cell trajectories. To study the effectiveness of cell separation a computational model has been developed in the COMSOL Multiphysics. No slip boundary condition is applied at the wall for the laminar flow and the bounce wall condition is applied for the particle tracing using the transient solver. A zero static pressure boundary condition is applied at the outlet. Grid independence study is performed with different built-in meshes and a grid with 523,734 elements is used. The computational model is verified against the experimental work of Ookawara et. al. [17].

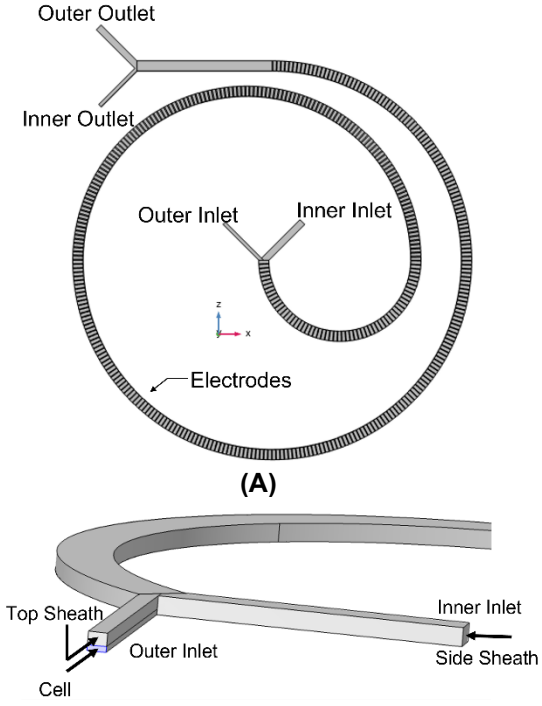

FIGURE 2: (A) SCHEMATIC OF THE ELECTRODE-EMBEDDED SPIRAL CHANNEL. (B) THE RELATIVE POSITION OF CELLS, TOP SHEATH AND SIDE SHEATH INLET HAVE BEEN SHOWN. CELLS AND THE TOP SHEATH HAVE BEEN INJECTED THROUGH THE OUTER INLET WHEREAS THE SIDE SHEATH HAS BEEN PUMPED THROUGH THE INNER INLET.

4. RESULTS AND DISCUSSION

In hybrid inertial microfluidic devices, DEP force plays a significant role in the separation of the CTCs from the binary mixture. The magnitude of the DEP force experienced by a cell largely determines the final equilibrium position of the cells and this magnitude is dependent on the dielectric properties of the cells and the buffer medium, the instantaneous position of the particle within the microchannel and the magnitude of the electric field strength. The magnitude of the electric field strength in turn depends on the applied voltage and the electrode configuration. In this study, the effect of voltage on the high-throughput separation is investigated. The influence of the sheath flow and electrode positioning is also discussed subsequently.

4.1 Effect of DEP on cell trajectories

As the binary cell mixture is carried by the buffer medium from the inlet to the outlet in the spiral microchannel, the CTCs are separated from the WBCs both vertically and laterally across the cross-section of the outlet. Trajectories of the WBCs and the CTCs are modeled in two different conditions: in the presence of an electric field and without an electric field. When there is no applied voltage, in the absence of an electric field, from Fig. 3A it can be seen that both the CTCs and the WBCs represented by the blue and the red streams respectively form a single stream and no separation of the cells can be observed. As the voltage is increased the CTCs do not change their trajectory as no DEP force acts on them whereas the WBCs start to migrate from the bottom of the channel to the top. There is a voltage above which no WBCs can be found at the bottom focusing position and this voltage is termed as critical voltage. For Re 30, 40, 50 and 60 the peak-to-peak critical voltage is 6, 7.5, 9.5, and 11V. At voltage above the critical voltage, all the WBCs are pushed vertically toward the top of the channel as can be seen from Fig. 4B.

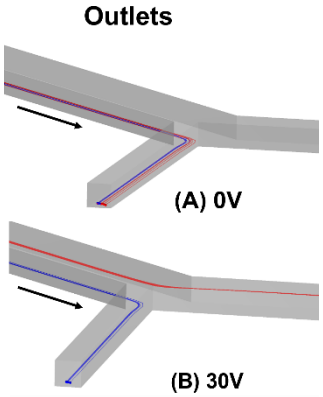

FIGURE 3: THE TRAJECTORY OF THE WBCS AND CTCS AT THE OUTLET ARE SHOWN BY THE RED AND BLUE LINES RESPECTIVELY FOR REYNOLDS NUMBER 60 AT (A) 0V (B) 30V.

4.2 Effect of the sheath flow

In a microfluidic channel embedded with interdigitated electrodes at the bottom of the channel, the strength of the non-uniform electric field decreases exponentially from the vicinity of the electrodes. As the strength of the electric field diminishes near the top of the channel, a top sheath flow needs to be employed to eliminate the top focusing position of the cells and push them near the bottom for their successful separation. In this work, several buffer inlet configuration for the top sheath flow has been explored as shown in Fig. 2B to study the impact of the sheath flow on the separation characteristics of the cells.

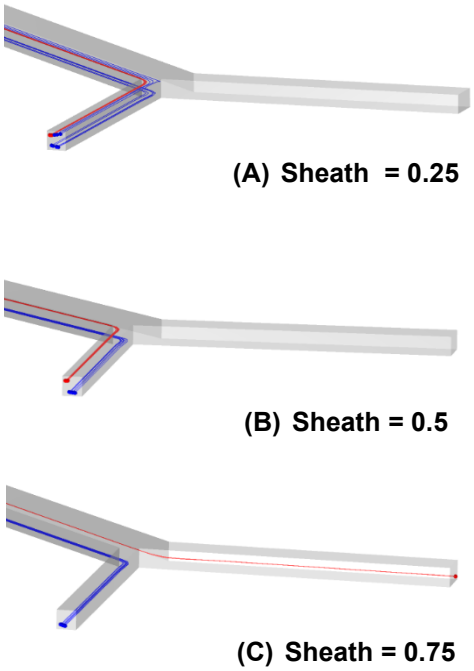

FIGURE 4: FOR AN APPLIED VOLTAGE OF 30V THE OUTLET POSITIONS OF THE CELLS WITH VARIATION IN THE TOP SHEATH DIMENSION [(A)0.25 (B) 0.50 (C) 0.75] ARE SHOWN IN THE FIGURE. THE RED STREAM REPRESENTS THE WBCS AND THE BLUE STREAM REPRESENTS THE CTCS.

The results show that in the absence of any DEP force when the applied voltage is zero and at the vertical buffer flow inlet of 25 µm, cells are found at approximately 20 µm and 80 µm of the channel height. Thus, two separate streams are formed with an identical mixture of cells. When the voltage is increased to the critical voltage no separation of the cells is observed. At a voltage greater than the critical voltage, it is observed that all the WBCs were moved to the top focusing position but the CTCs were distributed evenly between the top and bottom focusing positions as shown in Fig. 4A. Thus no distinct stream of WBCs and CTCs is found and the cell could not be separated in this configuration.

When the vertical buffer flow inlet is 50 µm, the cell mixture is pushed to the bottom half of the channel. At this configuration and in the absence of any electric field, only one focusing position of the cells is found at 20 µm from the bottom of the channel for both cell types, eliminating the top focusing position. As the voltage is increased, negative DEP force acts on the WBCs and they are pushed vertically upward. Owing to the dielectric properties of the CTCs no DEP force acts on them, hence the CTCs maintain their initial trajectory near the bottom of the channel. At a voltage greater than the critical voltage, two distinct streams of cells are formed represented by the blue and the red lines in Fig. 4B. At vertical buffer flow inlet of 75 µm, the WBCs and the CTCs are separated both vertically and laterally when the applied voltage is 30V. This can be employed to collect the CTCs and WBCs through different outlets as shown in Fig. 4C.

4.3 Effect of Reynolds number on separation

For any type of cell sorting device, the Reynolds number or throughput is a crucial parameter that determines the performance of the device. In this study, we have investigated the effect of Reynolds numbers ranging from 30-60 on the ability of the device to separate the different cell types. Fig. 5 shows the lateral and vertical height at which the WBCs are collected at the outlet. The CTCs have the same size as the WBCs, thus they are acted upon by the same inertial force, and hence they are observed to show a similar migration characteristic as WBCs at all the flow conditions. Additionally, the CTCs do not change their position at the outlet in the presence of an electric field and maintain their initial flow trajectory similar to the WBCs at 0V. As a result, the CTCs have been omitted from this figure.

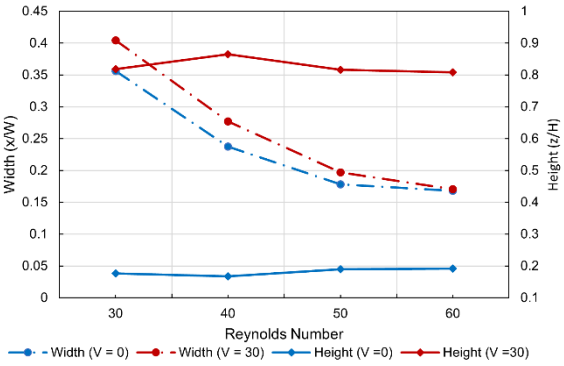

FIGURE 5: THE LATERAL AND VERTICAL POSITION OF THE WBCS AT THE OUTLET WITH THE VARIATION IN THE REYNOLDS NUMBER AT VOLTAGE 0 AND 30V GIVEN BY THE BLUE AND THE RED LINES RESPECTIVELY.

As the Reynolds number is increased, all the particles are pushed towards the side wall of the channel from the center due to the increase in the inertial-lift force. This is observed both in the presence and in the absence of an electric field and shown by the dashed lines in Fig. 5. Thus, with the increase in the Reynolds number, the lateral distance between the particles at the outlet decreases at 30V. However, it can be seen from the blue solid lines that the WBCs are found at the bottom of the channel when there is no applied voltage. In the presence of an electric field, when the applied voltage is 30V, significant DEP force acts on the WBCs, and as discussed in the previous section, the WBCs can be collected from the top of the channel as shown by the red solid line. As shown by both red and blue solid lines, the heights at which the WBCs are collected at the outlet do not change significantly with the Reynolds numbers. Thus, two separate streams of cells can be collected at the outlet.

5. CONCLUSION

In this study, the working mechanism of a hybrid inertial DEP device has been demonstrated for the separation of overlapping-sized CTCs from the WBCs. The effect of the electric field, sheath flow configuration, and flow rate have been studied numerically and the presented results show the successful separation of the CTCs from a binary mixture of cells. The results generated from this study will provide better guidelines for the development of high-throughput novel microfluidic cell separation devices and have the potential to impact how cancers are diagnosed through liquid biopsy.

ACKNOWLEDGEMENTS

X. L. Chen acknowledges the support from the National Science Foundation under grant NSF ECCS- 1917299.

REFERENCES

[1] Jemal, A., Bray, F., Center, M. M., Ferlay, J., Ward, E., and Forman, D., 2011, "Global Cancer Statistics," CA. Cancer J. Clin., **61**(2), pp. 69–90.

[2] Yang, C., Xia, B. R., Jin, W. L., and Lou, G., 2019, "Circulating Tumor Cells in Precision Oncology: Clinical Applications in Liquid Biopsy and 3D Organoid Model," Cancer Cell Int., **19**(1).

[3] Hayes, D. F., Cristofanilli, M., Budd, G. T., Ellis, M. J., Stopeck, A., Miller, M. C., Matera, J., Allard, W. J., Doyle, G. V., and Terstappen, L. W. W. M., 2006, "Circulating Tumor Cells at Each Follow-up Time Point during Therapy of Metastatic Breast Cancer Patients Predict Progression-Free and Overall Survival.," Clin. Cancer Res., **12**(14 Pt 1).

[4] Allard, W. J., Matera, J., Miller, M. C., Repollet, M., Connelly, M. C., Rao, C., Tibbe, A. G. J., Uhr, J. W., and

Terstappen, L. W. M. M., 2004, "Tumor Cells Circulate in the Peripheral Blood of All Major Carcinomas but Not in Healthy Subjects or Patients With Nonmalignant Diseases," Clin. Cancer Res., **10**(20), pp. 6897–6904.

[5] Jin, T., Yan, S., Zhang, J., Yuan, D., Huang, X. F., and Li, W., 2016, "A Label-Free and High-Throughput Separation of Neuron and Glial Cells Using an Inertial Microfluidic Platform," Biomicrofluidics, **10**(3).

[6] Dalili, A., Samiei, E., and Hoorfar, M., 2019, "A Review of Sorting, Separation and Isolation of Cells and Microbeads for Biomedical Applications: Microfluidic Approaches," Analyst, **144**(1), pp. 87–113.

[7] Gioe, E., Uddin, M. R., Kim, J. H., and Chen, X., 2022, "Deterministic Lateral Displacement (DLD) Analysis Tool Utilizing Machine Learning towards High-Throughput Separation," Micromachines 2022, Vol. 13, Page 661, **13**(5), p. 661.

[8] Di Carlo, D., 2009, "Inertial Microfluidics," Lab Chip, **9**(21), pp. 3038–3046.

[9] Marrinucci, D., Bethel, K., Lazar, D., Fisher, J., Huynh, E., Clark, P., Bruce, R., Nieva, J., and Kuhn, P., 2010, "Cytomorphology of Circulating Colorectal Tumor Cells: A Small Case Series," J. Oncol., **2010**, pp. 1–7.

[10] Rahmati, M., and Chen, X., 2021, "Separation of Circulating Tumor Cells from Blood Using Dielectrophoretic DLD Manipulation," Biomed. Microdevices, **23**(4).

[11] Church, C., Zhu, J., and Xuan, X., 2011, "Negative Dielectrophoresis-Based Particle Separation by Size in a Serpentine Microchannel," Electrophoresis, **32**(5), pp. 527–531.

[12] Zhu, J., Canter, R. C., Keten, G., Vedantam, P., Tzeng, T. R. J., and Xuan, X., 2011, "Continuous-Flow Particle and Cell Separations in a Serpentine Microchannel via Curvature-Induced Dielectrophoresis," Microfluid. Nanofluidics, **11**(6), pp. 743–752.

[13] Moon, H. S., Kwon, K., Kim, S. Il, Han, H., Sohn, J., Lee, S., and Jung, H. Il, 2011, "Continuous Separation of Breast Cancer Cells from Blood Samples Using Multi-Orifice Flow Fractionation (MOFF) and Dielectrophoresis (DEP)," Lab Chip, **11**(6), pp. 1118–1125.

[14] Zhang, J., Yan, S., Alici, G., Nguyen, N. T., Di Carlo, D., and Li, W., 2014, "Real-Time Control of Inertial Focusing in Microfluidics Using Dielectrophoresis (DEP)," RSC Adv., **4**(107), pp. 62076–62085.

[15] Khan, M., and Chen, X., 2022, "Numerical Study of Dielectrophoresis-Modified Inertial Migration for Overlapping Sized Cell Separation," Electrophoresis, **43**(7–8), pp. 879–891.

[16] Segré, G., and Silberberg, A., 1961, "Radial Particle Displacements in Poiseuille Flow of Suspensions," Nat. 1961 1894760, **189**(4760), pp. 209–210.

[17] Ookawara, S., Street, D., and Ogawa, K., 2006, "Numerical Study on Development of Particle Concentration Profiles in a Curved Microchannel," Chem. Eng. Sci., **61**(11), pp. 3714–3724.

[18] De Gasperis, G., Yang, J., Becker, F. F., Gascoyne, P. R. C., and Wang, X.-B., 1999, *Micro¯uidic Cell Separation by 2-Dimensional Dielectrophoresis*.

[19] Kim, D., Sonker, M., and Ros, A., 2019, "Dielectrophoresis: From Molecular to Micrometer-Scale Analytes," Anal. Chem., **91**(1), pp. 277–295.

[20] Cottet, J., Fabregue, O., Berger, C., Buret, F., Renaud, P., and Frénéa-Robin, M., 2019, "MyDEP: A New Computational Tool for Dielectric Modeling of Particles and Cells," Biophys. J., **116**(1), pp. 12–18.

[21] Prinyakupt, J., and Pluempitiwiriyawej, C., 2015, "Segmentation of White Blood Cells and Comparison of Cell Morphology by Linear and Naïve Bayes Classifiers," Biomed. Eng. Online, **14**(1), pp. 1–19.